Energetic Determinants of Internal Motif Recognition by PDZ Domains

Baruch Z. Harris, Brian J. Hillier,‡ and Wendell A. Lim*

Department of Cellular and Molecular Pharmacology, University of California, San Francisco, California 94143-0450

Received January 22, 2001; Revised Manuscript Received March 15, 2001

ABSTRACT: PDZ domains are protein−protein interaction modules that organize intracellular signaling complexes. Most PDZ domains recognize specific peptide motifs followed by a required COOH-terminus. However, several PDZ domains have been found which recognize specific internal peptide motifs. The best characterized example is the syntrophin PDZ domain which, in addition to binding peptide ligands with the consensus sequence -E-S/T-X-V-COOH, also binds the neuronal nitric oxide synthase (nNOS) PDZ domain in a manner that does not depend on its precise COOH-terminal sequence. In the structure of the syntrophin−nNOS PDZ heterodimer complex, the two PDZ domains interact in a head-to-tail fashion, with an internal sequence from the nNOS PDZ domain binding precisely at the peptide binding groove of the syntrophin PDZ domain. To understand the energetic basis of this alternative mode of PDZ recognition, we have undertaken an extensive mutagenic and biophysical analysis of the nNOS PDZ domain and its interaction with the syntrophin PDZ domain. Our data indicate that the presentation of the nNOS internal motif within the context of a rigid β-hairpin conformation is absolutely essential to binding; amino acids crucial to the structural integrity of the hairpin are as important or more important than residues that make direct contacts. The results reveal the general rules of PDZ recognition of diverse ligand types.

PDZ[1] domains are protein−protein interaction modules of approximately 100 amino acids that organize intracellular signaling complexes (for reviews, see refs *1*−*3*). Their name derives from the first three proteins in which they were discovered: PSD-95, Dlg-1, and ZO-1. Since their initial discovery, PDZ domains have been found in all eukaryotic organisms studied to date; 157 PDZ domains have been identified in the *Caenorhabditis elegans* genome, 208 in the *Drosophila melanogaster* genome, and 394 in the *Homo sapiens* genome (*4*, *5*). The most important function of PDZ domains appears to be in localization; many PDZ domains play an essential role in gathering receptors, channels, and downstream effectors at cell−cell communication junctions, as exemplified at neuronal synapses (*6*, *7*). Similarly, PDZ-containing proteins play a central role in regulating apical−basal polarity in epithelial cells (*8*).

PDZ domains mediate organization of signaling complexes by recognizing specific COOH-terminal amino acid sequence motifs (*9*). Specificity in PDZ domains is most commonly mediated through the recognition of a small number of amino acid side chains that are necessarily followed by a COOH-terminus (*10*). Peptide library studies show that the requirement for the carboxylate at the terminus is very stringent; addition or deletion of even one amino acid from the consensus sequence eliminates binding. Ligand sequence preferences of most PDZ domains can be divided into two major classes. Class I PDZ domains prefer the −S/T-X-Φ-COOH motif whereas class II PDZ domains the -Φ-X-Φ-COOH motif, where Φ is a hydrophobic amino acid. Recent work suggests that there are probably additional related recognition classes; some PDZ domains recognize unusual peptide sequences such as −D-X-V-COOH or -C-S-W-V-COOH (*11*, *12*), but these too require a COOH-terminus immediately following the consensus motif. Structural studies of PDZ−peptide complexes have revealed the interactions that determine sequence and COOH-terminus specificity (*13*−*15*). These structures show a series of binding pockets that recognize the P_{-2} and P_0 ligand residue side chains (where the P_0 site is defined as the most C-terminal residue of the peptide), as well as the terminal carboxylate ion. Backbone amides from the conserved "GLGF" loop in the PDZ domain combine with an ordered water molecule (bound by a conserved arginine or lysine) to form a network of hydrogen bonds that appears to hold the terminal carboxylate in place.

A growing body of evidence shows, however, that several PDZ domains can also recognize certain internal peptides (i.e., independent of a COOH-terminus), and that these internal interactions might be important in the assembly of signaling networks in vivo. The best evidence for internal ligand recognition comes from cases in which two PDZ domains heterodimerize. In these cases, a PDZ domain is able to bind another PDZ domain when it is expanded to

* To whom correspondence should be addressed: Department of Cellular and Molecular Pharmacology, University of California, San Francisco, CA 94143-0450. Phone: (415) 502-8080. Fax: (415) 502-8644. E-mail: wlim@itsa.ucsf.edu.

‡ Present address: Center for Marine Biotechnology and Biomedicine, Scripps Institute of Oceanography, University of California, San Diego, CA 92093-0202.

[1] Abbreviations: HPLC, high-pressure liquid chromatography; NMDA, *N*-methyl-D-aspartic acid; Ni−NTA, nickel−nitriloacetic acid; nNOS, neuronal nitric oxide synthase; PCR, polymerase chain reaction; PDZ, PSD-95, Discs-Large, ZO-1; PSD, postsynaptic density; SkM1, skeletal muscle type 1 sodium channel; TEV, tobacco etch virus.

10.1021/bi010142l CCC: $20.00
Published on Web 04/28/2001

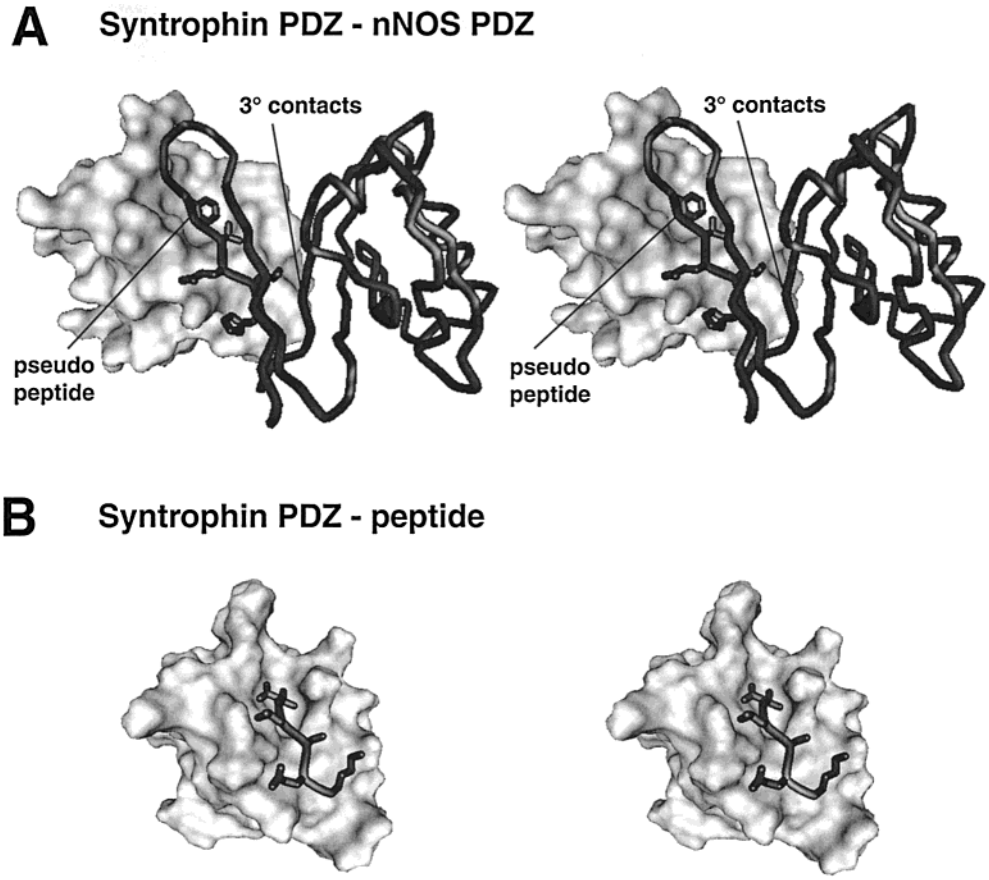

FIGURE 1: The same PDZ domain can bind two structurally distinct ligands. (A) Stereoview of the α1-syntrophin PDZ domain bound to the nNOS PDZ domain (residues 1−130) (from ref *20*). (B) Stereoview of the α1-syntrophin PDZ domain bound to the peptide -KESLV-COOH (from ref *29*). In both cases, syntrophin is shown as a white solvent-accessible surface (probe radius 1.7 Å) and the ligand is shown as a dark α-carbon trace. Side chains which make important contacts in the syntrophin PDZ domain binding pocket are shown in stick form. The "pseudopeptide" constitutes residues 106−111, with the sequence N-His-Leu-Glu-Thr-Thr-Phe-C.

include a small C-terminal extension, typically 20−30 amino acids. The best studied internal PDZ ligand is the neuronal nitric oxide synthase (nNOS) PDZ domain, which has a 30-amino acid extension that allows for heterodimerization with either the PDZ domain from α1-syntrophin or the second PDZ domain from PSD95 (both are class I PDZ domains) (*16*). These interactions, which do not involve C-terminal sequence motifs in either binding partner, are biologically important in localizing nNOS to the neuromuscular junction or the postsynaptic density, thereby allowing it to be activated by Ca^{2+} influxes that occur upon neuronal stimulation (*17*−*19*).

The finding of non-COOH-terminal PDZ ligands raises the question of how PDZ domains can recognize two such distinct ligands. The crystal structure of the nNOS−syntrophin PDZ heterodimer complex revealed that the extra 30 amino acids in nNOS fold into an unusual structure, a stable β-hairpin (termed the "β-finger") which binds at the same surface groove on the syntrophin PDZ domain as a COOH-terminal peptide ligand (*20*). Closer examination reveals that the β-finger of nNOS contains a near-consensus PDZ "pseudopeptide" sequence, that is, an internal peptide whose sequence and binding orientation closely resemble those of a canonical COOH-terminal peptide ligand (Figure 1). The nNOS pseudopeptide is immediately followed by a sharp type II β-turn, which occurs in place of the COOH-terminus found in peptide ligands. In addition, the syntrophin PDZ domain also contacts regions outside the pseudopeptide of nNOS; an extensive area of tertiary contacts occurs between the two core PDZ domains.

Little is known about the energetic determinants of the syntrophin−nNOS PDZ interaction. What is the affinity of this heterodimer interaction that involves recognition of an internal motif? How does it compare to the affinity of canonical peptide interactions? How does the nNOS PDZ domain overcome the apparent requirement for a COOH-terminus, observed for peptide ligands? Is it the presentation of the internal sequence in the proper secondary structural context (i.e., the β-finger) that allows for recognition, or do the additional tertiary contacts between the domains compensate for the lack of a carboxylate?

To better understand and compare the energetic mechanism of PDZ domain recognition of distinct ligand types, we have undertaken an extensive mutagenic analysis of both internal and COOH-terminal ligands. Using a solution binding method, we have been able to identify the key energetic determinants of the nNOS−syntrophin PDZ heterodimer interaction. Our results indicate that the structural context in which the internal "pseudopeptide" motif is presented is the primary determinant that allows the nNOS PDZ domain to bind the syntrophin PDZ domain. Residues that stabilize the β-hairpin topology of the nNOS β-finger are energetically as important (or more important) as residues that make direct side chain contact with the PDZ binding pocket. Surprisingly, in contrast, tertiary contacts between the two domains, away from the main binding groove, contribute little to the inter-

action energy. These studies suggest that recognition of internal sequences, if presented within the proper structural context, is probably a general mechanism of recognition for most PDZ domains.

EXPERIMENTAL PROCEDURES

Protein Expression and Purification. The nNOS, α1-syntrophin, and PSD95 PDZ domains were cloned, expressed, and purified as described previously (*20*). Briefly, PDZ domains from nNOS (residues 1−130), α1-syntrophin (residues 77−171), and PSD-95 (residues 149−253) were cloned from cDNA libraries using PCR with primers incorporating restriction sites at their 5′ ends. PCR products were gel purified, digested with appropriate restriction enzymes, and ligated into the expression vector pBH4, which incorporates an N-terminal His_6 tag and a cleavage site for the tobacco etch virus (TEV) protease. Proteins were expressed in *Escherichia coli* strain pLYS-S by growing cultures to an OD of 0.6−0.8 at 37 °C (for syntrophin and PSD-95 PDZ domains) or 25 °C (for the nNOS PDZ domain) and inducing with 1 mM IPTG for 3 h (for syntrophin and PSD-95) or 6 h (for nNOS). Cells from 6 L of culture were harvested by centrifugation, resuspended in 160 mL of 50 mM HEPES (pH 7.5) and 300 mM NaCl, and frozen at −80 °C. Subsequently, cell suspensions were thawed and lysed using a Branson model 250 sonifier. Lysates were cleared by centrifugation at 20000*g* and were incubated for 30−60 min at 4 °C with Ni^{2+}−NTA resin (Qiagen) with gentle rotation. The resin was collected by gentle centrifugation and transferred to a Bio-Rad Poly-Prep disposable column. Resin was washed twice with 50 mM HEPES (pH 7.5) and 300 mM NaCl and once with 50 mM NaH_2PO_4, 300 mM NaCl, and 10 mM imidazole. Bound protein was eluted with 50 mM NaH_2PO_4, 300 mM NaCl, and 250 mM imidazole and dialyzed overnight into 100 mM NaCl and 20 mM Tris-HCl (pH 7.4). The His_6 tag was, in some cases, removed by cleavage with ∼0.1 mg/mL TEV protease, followed by repurification as flow-through from a second Ni^{2+}−NTA resin column. In most cases, the nNOS mutant proteins were used in their His-tagged form, since the binding affinities for tagged and nontagged nNOS were found to be identical, and because there was a considerable decrease in yield upon TEV cleavage. The nNOS mutant proteins were purified directly by ion exchange. Protein solutions were dialyzed into the following buffers for ion exchange chromatography: 25 mM HEPES, 1 mM EDTA, and 10 mM NaCl (pH 7.0) for the α1-syntrophin PDZ domain, 25 mM MES and 1 mM EDTA (pH 6.0) for PSD-95 PDZ domain 2, and 25 mM NaOAc and 1 mM EDTA (pH 4.6) for the nNOS PDZ domain. All proteins were chromatographed on a 1 mL Resource S (Pharmacia) ion exchange column, eluting with a 0 to 1000 mM NaCl gradient in the corresponding buffer (above). Fractions containing protein were pooled and dialyzed into 20 mM HEPES (pH 7.0), and the purified protein was concentrated to 10−15 mg/mL (concentration assayed by absorbance at 280 nm) and frozen in liquid nitrogen in small aliquots. Individual aliquots were stored at −80 °C.

Synthesis and Modification of Peptides. Peptides were synthesized using conventional solid-phase Fmoc-amino acid chemistry on an ABI 381 synthesizer. Carboxylated peptides were synthesized using preloaded Wang resin (Novabiochem). Amidated peptides were synthesized using Rink-Amide resin (Novabiochem). Final deprotection was performed on the machine, and peptides were either N-terminally acetylated or dansylated on the resin as follows. For N-terminal acetylation, resin was incubated with an acetic anhydride/pyridine/dimethylformamide mixture (1:2:2) for 1 h, after which resin was washed with dimethylformamide and dichloromethane, dried over vacuum, and used in subsequent reactions. For N-terminal dansylation, a solution of 135 mg of dansyl chloride (Molecular Probes), 32 μL of diisopropylethanolamine, and 1.9 mL of dimethylformamide was added to ∼125 μmol of peptide equivalents on resin and the mixture incubated for 2 h at room temperature. Resin was then washed with dimethylformamide and dichloromethane and dried under vacuum. The reaction was repeated once and resin dried for cleavage. Cleavage from Rink-Amide and Wang resins was performed according to protocols provided by Novabiochem. Crude peptide solutions were precipitated with ether and lyophilized overnight, and then resuspended in 0.1% TFA with an amount of acetonitrile as small as necessary to solubilize the crude peptide. Peptides were purified on a Rainin Dynamax HPLC system using a Vydac 25 cm × 2.2 cm, 10 μm C18 column with a gradient of 0 to 90% acetonitrile in 0.1% TFA. Fractions corresponding to major peaks detected at 215 nm were lyophilized and redissolved in 0.1% TFA. The purity of fractions was assessed by HPLC on a Vydac 15 cm × 0.46 cm, 3 μm analytical C18 column; pure fractions were subsequently lyophilized, and a small amount was redissolved in buffer for electrospray mass spectrometry. The molecular masses of all peptides were verified to be within 0.5 Da by electrospray mass spectrometry, and final stocks were made in filtered deionized water at a concentration appropriate for binding experiments.

Mutagenesis of nNOS. The extended nNOS PDZ domain was mutated by a two-step PCR method. Overlapping primers were designed to anneal to opposite strands spanning the mutation site, and incorporated the mutation in their sequence. Two PCR half-reactions were performed, each with one of the internal mutagenic primers and another primer external to the cloning site. PCR products from both half-reactions were gel purified and used as templates for a second round of PCR, using only the external primers. The product of the second reaction was gel purified, cleaved with the appropriate restriction enzymes, and cloned into the pBH4 expression vector described above. Resulting plasmids were transformed into *E. coli* strain PLYS-S for expression, and proteins were purified exactly as described above for nNOS.

Measurement of Binding Affinities. Affinities for binding to PDZ domains were measured by two different methods. The binding of dansylated peptide ligands to PDZ domains was monitored by following the increase in fluorescence upon titration of a concentrated PDZ domain into a 1 cm × 1 cm stirred-cell cuvette containing 0.5 μM danyslated peptide ligand (starting volume of 1250 μL). The PDZ domain stock concentration was typically 1.5−2 mM, and the maximal volume of 45 μL was added in each experiment, corresponding to a final experimental PDZ concentration of ∼40 μM. Data were fit to the following equation (*21*) by nonlinear least-squares analysis using the program ProFit 5.1.0 (Quantum Soft):

$$y = F_o + \frac{(F_{max} - F_o)\frac{x}{K_d}}{1 + \frac{x}{K_d}}$$

where y is the fluorescence reading, x is the concentration of ligand (PDZ domain), K_d is the dissociation constant of the PDZ domain and peptide, F_o is the initial fluorescence value (fraction bound = 0), and F_{max} is the fluorescence value at saturation (fraction bound = 1).

For competition binding experiments using nonfluorescent ligands, 0.5 μM dansylated peptide was equilibrated with 0.25−2.5 μM PDZ domain in a total volume of 1250 μL. Under these conditions, given the K_d of the dansylated peptide ligand, the fraction of peptide bound was calculated to be 0.1−0.5. Unlabeled competitor ligand was then titrated into the cuvette, and the loss in dansyl fluorescence was monitored to follow displacement by the competitor. The change in fluorescence could be fit to the following equation (*22*):

$$F(c) = F_o\left\{1 + \left(\frac{F_{rel} - 1}{[L_o]}\right)\Big/_2\left[\left(\frac{K_d[C]}{K_c} + K_d + [L_o] + [P_o]\right) - \sqrt{\left(\frac{K_d[C]}{K_c} + K_d + [L_o] + [P_o]\right)^2 - 4[L_o][P_o]}\right]\right\}$$

where $F(c)$ is the fluorescence reading as a function of competitor concentration, [C] is the concentration of the competitor, F_o is the minimal fluorescence value ([C] = ∞), F_{rel} is the relative maximal fluorescence value at saturation, $[L_o]$ is the fluorescent peptide concentration, $[P_o]$ is the protein concentration, i.e., competition target, K_d is the dissociation constant of the peptide and competition target, and K_c is the dissociation constant of the competitor and competition target. This equation holds true as long as [C] ≫ $[L_o]$ and [C] ≫ $[P_o]$ and assumes the affinity of the competitor for the peptide ligand is negligible.

All competition binding experiments were performed in 50 mM HEPES (pH 7.5) and 50 mM NaCl at 20 °C. Each K_d value is the average of at least three independent experiments. For syntrophin PDZ domain binding to nNOS PDZ domain mutant proteins, a range of K_d values were observed, from as low as 0.26 μM for the nNOS ΔT112 mutant protein to as high as ∼199 μM for the nNOS F111A mutant protein. In practice, we found that the competition assay could be used to accurately measure dissociation constants when $K_d \leq 100$ μM. Most nNOS mutant protein binding affinities were also qualitatively verified using a GST-pulldown assay using the GST−syntrophin fusion protein as bait to pull down purified nNOS mutant proteins (data not shown).

CD Spectrometry. Circular dichroism spectrometry was performed on an AVIV model 62DS spectrometer. Wavelength scans were performed in a 0.1 cm × 1 cm quartz cuvette with samples in 25 mM potassium phosphate buffer (pH 7.5) and 10 mM KCl at 20 °C. Stability of most nNOS mutant proteins was assayed, as described previously (*23*), at least twice by following [Θ] at 222 nm during guanidine denaturation (data not shown) in a 1 cm × 1 cm stirred-cell quartz cuvette, with samples in 50 mM sodium phosphate buffer (pH 7.5) and 50 mM NaCl at 20 °C. With the exception of the I43A mutant protein, no mutant protein was found to have a >1 kcal/mol decrease in stability relative to wild-type nNOS residues 1−130. Wild-type stability to guanidine denaturation was measured by us to be ∼5.4 kcal/mol. Thus, under binding assay conditions, these mutant proteins are all >99.9% folded.

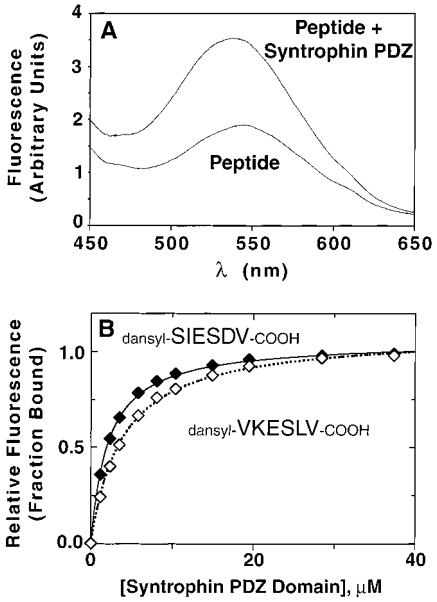

FIGURE 2: Direct solution binding of fluorescently labeled peptides to PDZ domains. (A) Emission scans of the dansylated peptide before and after addition of saturating amounts (40 μM) of the PDZ domain. (B) Binding isotherms of N-terminally dansylated PDZ ligand peptides to the α1-syntrophin PDZ domain (excitation at 330 nm; emission at 540 nm). Data were normalized as "fraction bound" such that the initial fluorescence = 0 and the fluorescence at saturation = 1. Solid lines are best fits to experimental data (see Experimental Procedures).

RESULTS

Fluorescence-Based Solution Binding Assays for PDZ Interactions. To quantitate the affinities of binding of various ligands to PDZ domains, we developed a fluorescence-based binding assay. We first synthesized peptide ligands that were modified at their NH_2-termini to contain a dansyl group. The fluorescence intensity of this compound is highly sensitive to local environment and often increases upon binding to a protein ligand, due to reduction of the level of quenching from surrounding water molecules. The purified PDZ domain (either the syntrophin or PSD-95 domain) was then titrated into a cuvette containing an NH_2-terminally dansylated peptide ligand. As shown in Figure 2, the increase in fluorescence intensity observed with increasing PDZ concentration can be fit to a simple 1:1 bimolecular binding reaction with a dissociation constant (K_d) in the micromolar range. It should be noted that, at least for these specific PDZ−peptide pairs, these are the first direct solution binding measurements of PDZ interaction affinities. Previous results, primarily using solid-phase assays such as ELISA or surface plasmon resonance, appear to have often resulted in considerable overestimates (often into the low nanomolar range) for the interaction affinity.

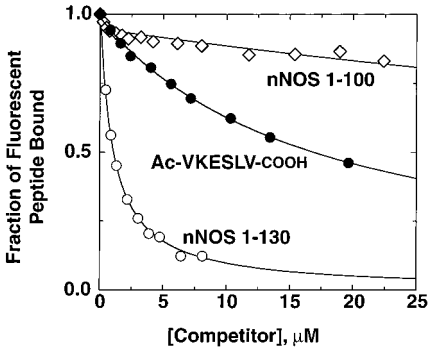

FIGURE 3: Fluorescently labeled peptides can be used to measure affinities of nonfluorescent PDZ ligands via competition. Competition binding curves against the α1-syntrophin PDZ domain are shown. Data are normalized to fraction of fluorescent peptide bound such that initial values = 1 and saturating values = 0. Solid lines are best-fit curves (see Experimental Procedures). For reference, nNOS residues 1−100 make up the canonical (lacking the β-finger) PDZ domain, and nNOS residues 1−130 make up the PDZ domain (inclusive of the β-finger).

Competition Binding Assay. Once reliable binding affinities had been established for these PDZ−dansyl peptide pairs, we proceeded to use competition methods to measure solution binding affinities for a wider range of PDZ ligands that were not fluorescently labeled. Figure 3 shows sample competition binding curves obtained from such experiments. We found that nonfluorescent peptides competed effectively with the equivalent dansylated peptides for PDZ domain binding, although their affinity is ~2-fold lower. The slightly higher affinity of the fluorescent peptides may be due to favorable interactions between the PDZ domain and the hydrophobic dansyl group. Peptide binding data obtained from competition (as well as direct binding) experiments are summarized in Table 1.

Using the competition binding assay, the nNOS PDZ domain was found to bind to the syntrophin PDZ domain with a dissociation constant of 0.6 μM (Figure 2 and Table 2). In the same assay, the second PDZ domain from PSD-95 bound with a dissociation constant of 4.5 μM (data not shown). Thus, the nNOS domain binds to the syntrophin domain with an affinity approximately 10-fold higher than that of canonical peptide ligands; the nNOS domain binds to the PSD95 domain with an affinity approximately equal to that of peptide ligands. As predicted from previous studies (*16*), the affinity of nNOS for its cognate PDZ domain was dramatically reduced (by >200-fold, $\Delta\Delta G$ > 3.0 kcal/mol) upon removal of the 30-amino acid β-finger.

Affinity of Peptide Ligand Variants. We used the solution competition binding assay to analyze the energetic contribution of key residues in COOH-terminal peptide ligands. As a model peptide, we used the sequence VKESLV-COOH, which is derived from the mammalian protein SkM1 and

Table 1: Affinities of Binding of Selected Peptides to α1-Syntrophin and PSD-95 (#2) PDZ Domains

	Binding to:	A. α1-Syntrophin PDZ Domain		B. PSD-95 PDZ Domain #2	
position[a]					
P_{-5} P_{-4} P_{-3} P_{-2} P_{-1} P_0 P_{+1} P_{+2}		K_d (μM)	ΔG (kcal/mol)[c]	K_d (μM)	ΔG (kcal/mol)
I. Direct Binding (N-terminally dansylated peptides)					
S I E S D V[b]		2.1 (±0.1)	-7.6 (±0.0)	1.8 (±0.2)	-7.7 (±0.0)
V K E S L V		3.4 (±0.2)	-7.3 (±0.0)	1.9 (±0.8)	-7.7 (±0.3)
II. Competition Binding					
S I E S D V		7.4 (±0.9)	-6.9 (±0.1)	3.7 (±0.4)	-7.3 (±0.0)
V K E S L V		7.6 (±1.8)	-6.9 (±0.1)	4.8 (±0.6)	-7.1 (±0.0)
V K E A L V		54 (±2.2)	-5.7 (±0.0)	18 (±1.9)	-6.4 (±0.1)
V K E S L A		64 (±1.6)	-5.6 (±0.0)	83 (±13)	-5.5 (±0.1)
V K E S L V	-$CONH_2$	>100	> -5.4	>100	> -5.4
H L E T T F		31 (±2.5)	-6.1 (±0.0)	30 (±1.9)	-6.1 (±0.0)
H L E T T F	-$CONH_2$	>100	> -5.4	>100	> -5.4
H L E T T F T G	-$CONH_2$	>100	> -5.4	>100	> -5.4
··· H L E T T F ···	*(nNOS 1-130)*[d]	0.61(±0.05)	-8.3(±0.1)	4.5 (±0.4)	-7.2 (±0.1)

[a] Peptide binding positions are defined as described in ref *8*, where P_0 is the carboxy-terminal amino acid. [b] All peptides terminate with a -COOH group, unless otherwise indicated. [c] Values in parentheses are standard deviations derived from at least three independent experiments. ΔG values were calculated from individual K_d values. [d] Values in this row correspond to affinities for nNOS residues 1−130, a fragment which contains the sequence -HLETTF- as an internal motif. Peptides derive from the following proteins: SIESDV, Skm1; VKESLV, NMDA receptor subunit 2B; and HLETTFTG, nNOS pseudopeptide motif.

Table 2: Affinities of Binding of the nNOS PDZ Domain (residues 1−130) and Mutant Proteins to the α1-Syntrophin PDZ Domain

nNOS variant	relative affinity ($K_d$mut/K_dWT)	$\Delta\Delta G_{binding}$[b]
WT (nNOS residues 1−130)[a]	1.0 ± 0.1	−
nNOS residues 1−100	>100	>3.0
direct contact mutants		
I. pseudopeptide		
T109A	42.8 ± 11.7	2.2 ± 0.2
F111A	>100	>3.0
F111V	0.3 ± 0.0	−0.6 ± 0.0
F111L	8.2 ± 1.0	1.2 ± 0.0
II. tertiary contacts		
P13A	1.5 ± 0.2	0.2 ± 0.1
V15A	0.8 ± 0.0	−0.2 ± 0.0
S17A	1.1 ± 0.0	0.0 ± 0.0
R19A	1.7 ± 0.0	0.3 ± 0.0
structural mutants		
I. β-turn		
ΔT112	0.4 ± 0.1	−0.5 ± 0.1
T112A	1.5 ± 0.0	0.3 ± 0.0
G113A	6.5 ± 0.1	1.1 ± 0.0
D114A	1.3 ± 0.1	0.2 ± 0.0
G115A	0.5 ± 0.0	−0.4 ± 0.0
G113A/G115A	0.9 ± 0.2	−0.1 ± 0.1
insertion series (between T112 and G113)		
1-Ala	0.7 ± 0.0	−0.25 ± 0.0
2-Ala	1.3 ± 0.1	0.14 ± 0.1
3-Ala	1.5 ± 0.2	0.26 ± 0.1
4-Ala	2.6 ± 0.1	0.56 ± 0.0
6-Ala	2.8 ± 0.1	0.61 ± 0.0
8-Ala	3.1 ± 0.3	0.67 ± 0.1
10-Ala	7.6 ± 0.3	1.18 ± 0.0
II. overall hairpin topology		
I43A (PDZ core)	39.6 ± 4.1	2.2 ± 0.1
R121A (β-finger clasp)	>100	>3.0

[a] The absolute K_d of nNOS for syntrophin is 0.61 ± 0.05 μM. [b] Values in parentheses are standard deviations derived from at least three independent experiments. ΔG values were calculated from individual K_d values.

binds both PSD-95 and syntrophin. Specifically, we wanted to evaluate the energetic contribution of the P_0 and P_{-2} positions, which have been found to be important for binding; we therefore mutated each of these residues to alanine. We also wanted to evaluate the energetic importance of the terminal COOH group in peptide binding, and tested this by chemically modifying the C-terminal carboxylate (COOH) to a carboxamide ($CONH_2$). Mutation of either P_0 or P_{-2} residues to alanine significantly affects binding by up to 1.7 kcal/mol. Modifying the terminal carboxylate to a carboxamide, however, results in an even more dramatic decrease in binding energy (>3.0 kcal/mol), indicating that, at least in the peptide ligand, the carboxylate contributes a significant portion of the binding energy.

We also evaluated the specificity of the PSD-95 and syntrophin PDZ domains by testing them both for binding to multiple peptide sequences (Table 1). In addition to the Skm1 peptide, we assessed binding of these domains to the NR2B peptide from NMDA receptor subunit 2B (SIESDV-COOH), which was identified as a PSD95 ligand (*16*), and a peptide derived from the pseudopeptide sequence of the nNOS PDZ domain (HLETTFTG). Surprisingly, none of these peptides appear to bind with notable preference for either of the two tested PDZ domains. Both biologically relevant peptide ligands bind to both PDZ domains with micromolar dissociation constants. The pseudopeptide fragment from nNOS shows detectable but weak binding to both test PDZ domains. These measurements show that when the pseudopeptide is placed in the context of the full nNOS PDZ domain, its binding to the syntrophin PDZ domain is enhanced by >50-fold. It is striking, however, that in the peptide context, appending even a few additional carboxyl terminal residues or modifying the terminus to an amide completely abolishes binding.

Mutation of "Direct Interaction" Residues in the nNOS PDZ Domain. To dissect the mechanism of the syntrophin PDZ domain recognition of the nNOS PDZ domain, we first examined the energetic role of residues that lie at the interface between the two domains. These residues, involved in direct interactions observed in the complex crystal structure, can be subdivided into two categories. The first category is made up of those residues in the nNOS PDZ domain that form the pseudopeptide, the stretch of sequence that inserts into the canonical PDZ peptide binding groove of syntrophin. The second category is made up of those residues that lie outside of the pseudopeptide and participate in direct "tertiary" interactions with regions on the syntrophin PDZ domain outside of its canonical binding groove. These tertiary interactions cover approximately 266 Å^2 of the solvent-accessible surface area on the nNOS domain, compared to the total of ∼800 Å^2 occluded in the entire interface. It is possible that these additional tertiary interactions may allow the extended nNOS PDZ domain to compensate for the loss of energy resulting from the lack of a carboxy terminus.

The role of residues in the pseudopeptide and the tertiary interaction surface was evaluated by alanine scanning mutagenesis coupled with measurements of the resulting change in the free energy of binding. The effects of these two classes of direct interaction mutant proteins, measured using our competition binding assay, are summarized in Figure 4.

As expected, mutations of the consensus P_{-2} and P_0 residues in the pseudopeptide to alanine (T109A and F111A, respectively) have very strong unfavorable effects on binding ($\Delta\Delta G$ > 2 kcal/mol), indicating that these residues and their interactions play a critical energetic role. The energetic effects of alanine substitutions at the P_{-2} and P_0 sites closely mirror the effects observed when similar mutations are made in the context of the carboxy-terminal peptides ligands. It is noteworthy, however, that we find that the hydrophobic residue at the terminal P_0 site (position 111 in the nNOS pseudopeptide) is able to tolerate a surprising degree of side chain variability; Phe,Val, or Leu can all be tolerated, with the valine substitution yielding an even higher affinity than the wild-type phenylalanine residue. Thus, mutation of the nNOS pseudopeptide to a sequence that more closely matches the consensus peptide recognition motif for the syntrophin PDZ domain (-S/T-X-V-COOH) results in a gain of >0.5 kcal/mol in binding energy. While this suggests that the pseudopeptide is recognized in a manner generally similar to that of COOH-terminal peptides, the requirement for valine at the P_0 position is clearly far more stringent in the context of the free peptide interaction. The difference in P_0 site specificity probably reflects the fact that the peptide backbone of the nNOS pseudopeptide is displaced somewhat further away from the syntrophin PDZ domain surface than is observed in PDZ−peptide complexes.

To test the energetic role of nNOS residues outside of the pseudopeptide, we focused on four residues that make the

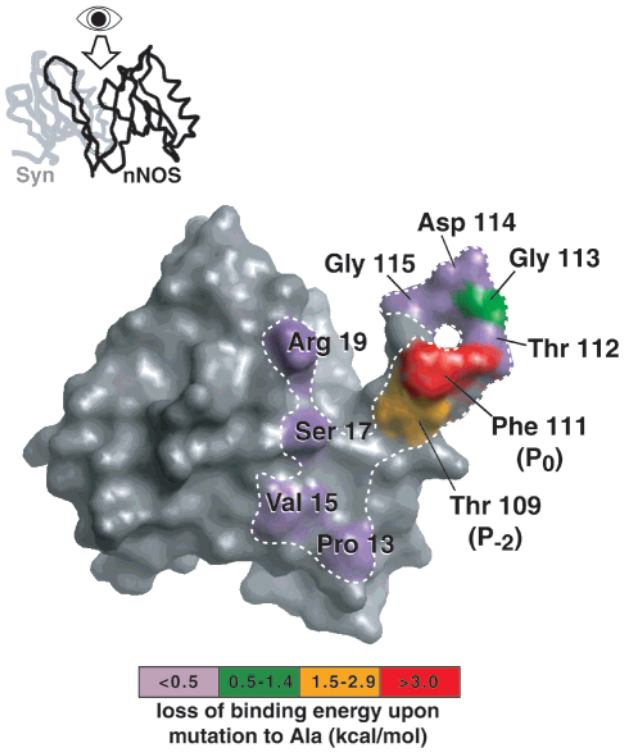

FIGURE 4: Energetically critical residues at the nNOS−syntrophin binding interface. nNOS is shown as a gray solvent-accessible surface area (probe radius of 1.7 Å); the syntrophin PDZ domain contact "footprint" is marked with a white dotted line. Residues that contact the syntrophin PDZ domain are colored according to the effect of the corresponding mutation (color scheme at bottom). A schematic of the nNOS−syntrophin structure is shown (top left) to indicate the orientation of the figure, which has been rotated 180° around the vertical axis relative to Figure 1.

bulk of the remaining tertiary contacts with the syntrophin PDZ domain: Pro-13, Val-15, Ser-17, and Arg-19. All four of these residues exhibit >30 Å^2 decreases in solvent accessibility when comparing the structure of nNOS alone with that of the nNOS−syntrophin PDZ complex. Arg-19, in particular, forms an intermolecular salt bridge with syntrophin residue Asp-143.

Despite their extensive interactions, these tertiary contact residues appear to play only a minor energetic role in binding. Mutation of any of these residues to alanine has only small effects on the strength of the interaction (ΔG < 0.4 kcal/mol), and some mutations actually increase the binding energy. Thus, in contrast to the pseudopeptide residues, these tertiary contact residues are not a major determinant of binding. This assertion is further supported by the previously reported finding that short (11-residue) peptides containing an internal consensus peptide recognition motif, when cyclized with a disulfide bond, are also competent to bind PDZ domains (*24*). We have measured the dissociation constant of such a cyclic peptide for the syntrophin PDZ domain to be 1.5 ± 0.1 μM, which is only slightly less favorable than binding of the syntrophin PDZ domain to the nNOS PDZ domain.

Mutation of "Structural" Residues in the nNOS PDZ Domain. The pseudopeptide of the nNOS PDZ domain is presented in a highly unusual secondary structure. The consensus recognition motif lies at the tip of a highly extended β-hairpin, which we term the β-finger of nNOS. The β-finger appears to be quite rigid, as it maintains its extended conformation even in the crystal structure of the nNOS PDZ domain alone. Moreover, Wang et al. (*25*) have found that the β-finger peptide alone, even when removed from the core nNOS PDZ domain, may retain some residual hairpin structure.

To evaluate the role of this unusual structural presentation in the interaction between the syntrophin and nNOS PDZ domains, we mutated several residues in nNOS that were hypothesized to play a role in stabilizing the β-finger. These structural residues fell into two categories. The first category consists of residues important for the formation of the type II β-turn at the tip of the β-finger. This sharp turn assumes the position normally occupied by the carboxylate of canonical peptide ligands. Moreover, in the syntrophin−nNOS PDZ complex structure, one of these residues (Gly-113) adopts a glycine-only set of ϕ and ψ angles. The second category of structural residues is made up of those that appear to stabilize the overall β-hairpin topology of the finger. One example is Arg-121, which is at the C-terminal base of the β-finger and participates in a buried salt bridge with Asp-62, a highly conserved residue within the main PDZ domain. The Arg-121−Asp-62 salt bridge appears to act as a "clasp", pinning back the C-terminal end of the β-finger to the core PDZ domain and potentially stabilizing the hairpin topology. Other residues that may be structurally important for the overall β-hairpin topology are those that are necessary for proper folding of the core PDZ domain, since the β-finger structure appears to be built upon interactions with this folded domain scaffold.

The effects of mutating the structural residues, summarized in Figure 5, indicate that stabilization of the nNOS β-finger conformation is a critical element in its recognition by the syntrophin PDZ domain. The most striking evidence in support of this role is the fact that disruption of the Arg-121−Asp-62 salt bridge in nNOS, which acts as a clasp stabilizing the β-finger, completely eliminates recognition by the syntrophin PDZ domain as detected by our assay ($\Delta\Delta G$ > 3.0 kcal/mol). The CD spectrum of this mutant protein is identical to that of wild-type nNOS residues 1−130, showing that the R121A mutation does not cause global unfolding of the nNOS domain (Figure 5B). A similar result was observed by Tochio et al. for the nNOS−PSD-95 PDZ heterodimer interaction (*26*). A second piece of evidence which shows that the structure of the β-finger is critical for recognition is the finding that mutation of a residue in the hydrophobic core of the main nNOS domain (I43A) also reduces the binding affinity by >40-fold ($\Delta\Delta G$ > 2.2 kcal/mol). In this case, the I43A mutation appears to globally destabilize the entire nNOS PDZ domain (Figure 5). This finding supports the model in which the structure of the main PDZ domain is required to stabilize the β-finger, which in turn is required for proper recognition.

The residues in the actual β-turn at the tip of the β-finger play an important role in the interaction, although this role is of a lesser magnitude than that of the structural residues described above. Particularly, mutation of glycine 113, which in the complex structure adopts a unique glycine-only set of ϕ and ψ angles, resulted in ~1 kcal/mol loss in binding affinity. Oddly, however, mutation of glycine 115 to Ala results in a slight increase in binding affinity. To more directly explore the role of the nNOS β-turn in recognition,

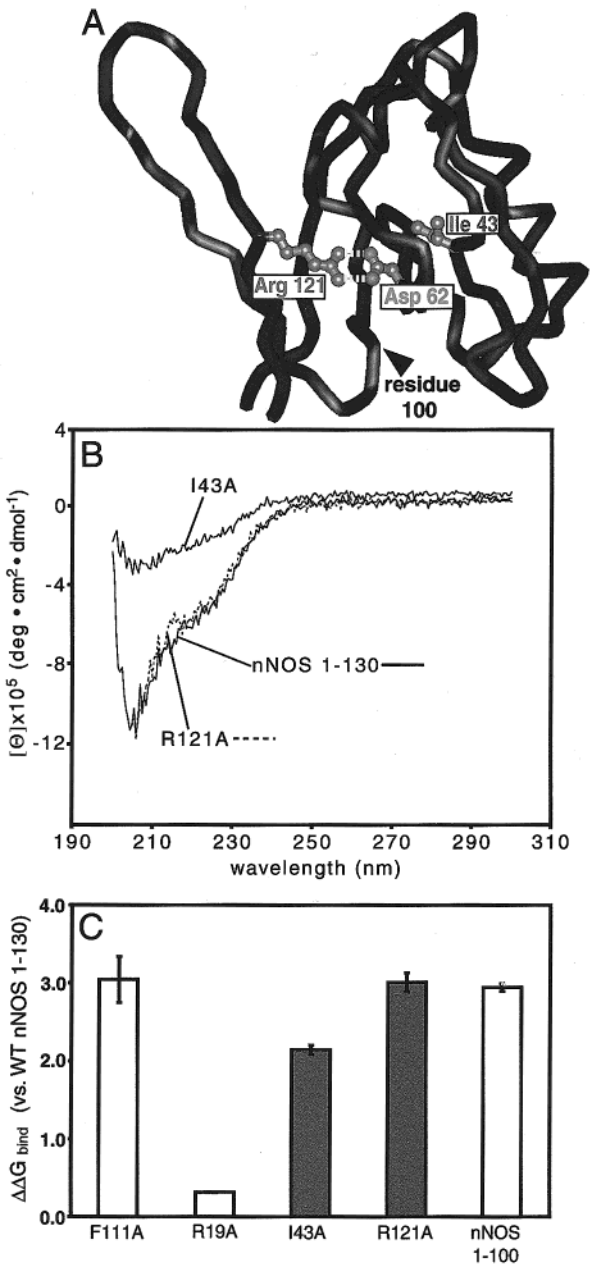

FIGURE 5: Residues that stabilize the β-finger structure in nNOS residues 1−130 are crucial for recognition by the syntrophin PDZ domain. (A) A schematic of the nNOS structure alone, oriented as in Figure 1. Side chains of relevant residues are labeled and shown in ball-and-stick form. (B) Circular dichroism spectra of wild-type nNOS residues 1−130, the R121A mutant, and the I43A mutant (all collected at 20 μM). (C) Energetic effects of the above mutations on the nNOS−syntrophin interaction (shaded bars). Mutations in direct contact residues that have a large (F111A) or negligible (R19A) effect are shown for reference (white bars). Error bars represent standard deviations from three independent experiments.

we also generated a set of insertion mutants, in which we added from 1 to 10 additional alanine residues between threonine 112 and glycine 113 in nNOS. The effects of these insertion mutants, summarized in Figure 6, illustrate that the β-turn has a modest tolerance for additional residues. However, there is a direct correlation between the number of inserted residues and the loss of binding affinity such that an insertion of 10 alanine residues results in a >1 kcal/mol decrease in binding energy. Together, these results indicate the β-turn must be relatively small for the preceding

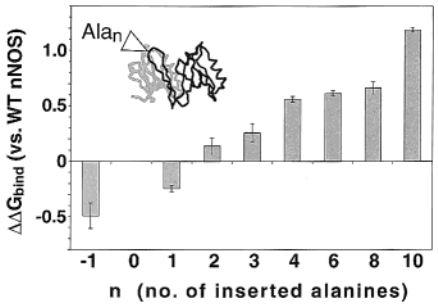

FIGURE 6: Insertions in the tip of the nNOS β-hairpin (residues 1−130) progressively destabilize binding to the syntrophin PDZ domain. $\Delta\Delta G$ values for binding are shown relative to that of wild-type nNOS residues 1−130, with n being the number of alanine insertions between residues T112 and G113. An n of −1 corresponds to ΔT112, and an n of 0 corresponds to the wild type. The total range of observed $\Delta\Delta G$ values is 1.7 kcal/mol. Error bars represent standard deviations from three independent experiments.

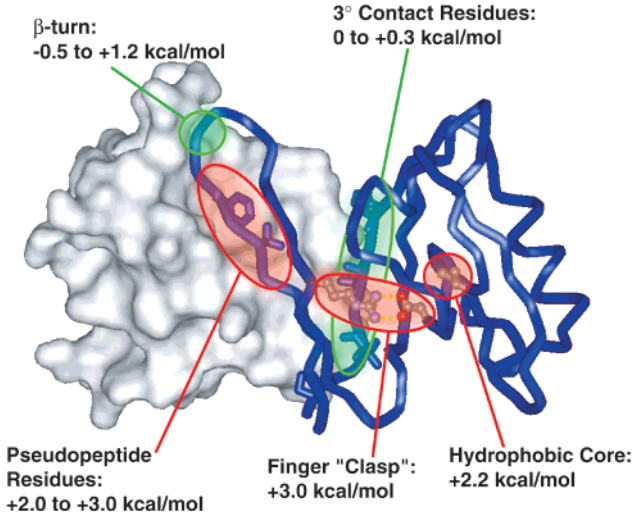

FIGURE 7: Summary of the overall effects of mutations in the nNOS PDZ domain on its affinity for the α1-syntrophin PDZ domain. The range of $\Delta\Delta G$ values for each type of mutation is shown at the corresponding location, indicating the magnitude of the effect. Residues or regions that have major effects (≥1.5 kcal/mol) are shaded in red; residues that have minor effects (<1.5 kcal/mol) are shaded in green. Highlighted residues are as follows: β-turn residues Thr-112, Gly-113, Asp-114, and Gly-115; tertiary contact residues Pro-13, Val-15, Ser-17, and Arg-19; pseudopeptide residues Thr-109 and Phe-111; finger clasp residues Asp-62 and Arg-121; and hydrophobic residue Ile-43.

pseudopeptide sequence to be properly recognized. However, the precise sequence, size, and, presumably, conformation of the β-turn are not critical for recognition.

DISCUSSION

We have presented an analysis of the nNOS−syntrophin PDZ−PDZ heterodimer interaction, with the aim of identifying the key energetic determinants that allow for PDZ-mediated recognition of an internal sequence motif. We are specifically interested in understanding how a single binding surface on a PDZ domain can be used to recognize two distinct ligand types: both specific peptide motifs followed immediately by a carboxy terminus, as well as internal motifs, as in the case of the nNOS−syntrophin interaction. Starting with the crystal structure of this complex, we have used site-specific mutagenesis to test various hypotheses concerning the driving force of this noncanonical PDZ

interaction. From this analysis, a general model for PDZ domain recognition emerges which can coherently explain both carboxy-terminal and internal motif recognition.

Energetically Critical Contacts Are Concentrated in the nNOS Pseudopeptide Motif. Two general regions on the extended nNOS PDZ domain are involved in direct contacts with the syntrophin PDZ domain. The first is the pseudopeptide motif that occurs on the tip of the nNOS extended β-finger and which inserts into the peptide binding groove of the syntrophin domain. The second region is comprised of residues in the main nNOS PDZ domain which make tertiary contacts with regions on the syntrophin domain surrounding the peptide binding groove. These interactions are only observed in an internal motif ligand like nNOS, and are absent in recognition of carboxy-terminal peptides.

Our results show that the bulk of the energy driving recognition between the syntrophin and nNOS PDZ domains involves residues in the pseudopeptide motif of nNOS. First, mutation of the key pseudopeptide residues essentially eliminates binding. Second, mutation of tertiary contact residues has very minimal effects on the interaction. Thus, these additional contacts do not appear to compensate for the lack of a carboxylate in the nNOS internal ligand. Together, these results show that the mechanisms by which carboxy-terminal and internal motifs are specifically recognized are analogous. The pattern of sensitivity to mutations for both ligands is very similar. Although the interaction interface for the PDZ−PDZ complex is considerably larger, the same core peptide motif constitutes a "hotspot" for binding energy. There does not appear to any specific, direct interaction that compensates for the lack of a C-terminal carboxylate in the nNOS internal ligand.

Proper Structural Presentation Is Essential for Internal Motif Recognition. Although the energetically important direct contacts in the syntrophin−nNOS PDZ−PDZ interaction primarily involve the nNOS pseudopeptide residues, other residues in nNOS play a critical but indirect energetic role in recognition. Our results suggest that the structural context in which the pseudopeptide is presented is as important as the sequence of the pseudopeptide itself. The extended nNOS PDZ domain appears to be a highly ordered scaffold that properly presents the internal pseudopeptide motif to the syntrophin PDZ domain. In particular, we have identified two structural mutations in nNOS that are as detrimental to binding as mutation of the pseudopeptide residues or complete truncation of the β-finger. First, we find that disruption of the overall nNOS PDZ fold, through mutation of the hydrophobic core residue isoleucine 43 to alanine, results in a 2.2 kcal/mol loss in binding free energy. Second, we find that arginine 121 is critical for binding, despite the fact that it does not directly contact the syntrophin PDZ domain. In the structure, arginine 121, which is at the end of the nNOS β-finger, forms a salt bridge with aspartate 62 in the main nNOS PDZ domain. This pair of residues thus appears to act as a clasp that pins back the end of the finger to the main PDZ domain. Together, these structural and energetic findings suggest that loss of this clasp interaction results in a loss of the rigid and extended β-finger required for proper presentation of the internal pseudopeptide motif.

We also find that residues in the sharp β-turn at the tip of the nNOS β-finger play an important role in binding. Mutation of glycine 113, which in the complex adopts "glycine-only" ϕ and ψ torsional angles, results in a moderate loss in affinity. We also find that insertion of additional residues in the turn results in a gradual decrease in binding energy that correlates well with the number of inserted residues. The results of the β-turn mutagenesis suggest that the ability to form a sharp β-turn at the end of the nNOS β-finger contributes to recognition. However, the exact nature of the turn residues is not critical and therefore does not constitute a rigid set of sequence requirements.

Taken together, our data indicate that the extended nNOS PDZ domain provides a structural context for a short internal amino acid sequence motif (the pseudopeptide) which satisfies the binding requirements for the PDZ domain. These findings are consistent with previous studies in which it was found that the syntrophin PDZ domain could recognize internal motifs present in peptides cyclized by an internal disulfide linkage (*24*). Recognition in this case was also dependent on proper structural presentation, as reduction of the cyclic disulfide linkage eliminated binding.

General Rules of PDZ-Mediated Protein−Protein Recognition. On the basis of our work, we are able to establish a set of general rules that can explain PDZ domain recognition of both carboxy-terminal and internal motifs. First, either class of ligands must contain the proper core linear amino acid recognition motif. The side chains in both types of syntrophin ligands maintain the required -E-S/T-X-Φ- motif that inserts into the PDZ binding groove and makes most of the energetically critical interface contacts. Second, these residues must be followed by either a carboxyl terminus or, alternatively, a stabilized β-turn. Although a β-turn could be stabilized through many different types of sequences and interactions, in the case of nNOS we find that turn-favoring residues and a clasp-like salt bridge interaction contribute significantly to stabilizing the conformation compatible with recognition. It is to be expected that similar clasp-like interactions will be required to pin back other internal PDZ ligands. However, this type of topological interaction need not be identical to the salt bridge observed in nNOS; clasp interactions could be highly degenerate and, as a result, difficult to identify from sequence alone.

The structural and energetic similarity observed between both modes of PDZ interactions suggests that recognition of internal motifs is probably a general mode of PDZ domain function; it does not appear to involve any unique features of the syntrophin PDZ domain, but rather is primarily determined by the unique structural context in which the nNOS pseudopeptide ligand is presented. These types of internal motifs are probably more rare and therefore harder to identify. Nonetheless, a number of recent papers have shown evidence to support the idea that PDZ−PDZ dimerization or oligomerization is a widespread phenomenon. Xu et al. showed that the third and fourth PDZ domains of the *D. melanogaster* protein INAD can heterodimerize, and that this interaction is dependent on a 28-amino acid C-terminal extension to the third PDZ domain (*27*). In addition, Fouassier et al. (*28*) have recently shown that the two PDZ domains from the human protein EBP50 (also known as NHERF) can homo- or heterodimerize. The PDZ domains used in this study also contained additional C-terminal sequences of ~30 amino acids. A brief inspection of the sequences of the C-terminal extensions in EBP50 shows

sequences that are similar to the nNOS β-finger in some ways; however, more detailed studies must be carried out to elucidate the specific mechanism of heterodimerization. The C-terminal extension in INAD bears little resemblance to that of the nNOS β-finger; however, it consists mainly of charged residues such as lysine and glutamate. Whatever the mechanism of heterodimerization in these systems and others, it is tempting to speculate that all PDZ domains have the capability to recognize not only C-terminal amino acid sequence motifs but also properly presented internal sequences, and that these interactions play an important role in signaling.

Although these findings suggest that internal recognition motifs for PDZ domains are likely to be difficult to identify from sequence analysis alone, a converse implication of these findings is that PDZ domains may be a more useful target for drug design than previously thought. If the negatively charged carboxylate ion of PDZ ligands were absolutely essential for binding, then it would be difficult to obtain small molecule inhibitors that could both bind PDZ domains and be cell permeable. However, these findings suggest that particular conformational scaffolds can eliminate the requirement for the carboxylate ion. Understanding exactly what types of scaffolds are able to do this may allow for the development of potent and useful inhibitors of PDZ domain-mediated interactions.

ACKNOWLEDGMENT

We thank C. Turck and C. Bui in the Turck lab for assistance with peptide synthesis and mass spectrometry. We also thank R. Zuckerman and Chiron Technologies for Amino Acid Analysis, A. Frankel for use of the CD spectrometer, and R. Bhattacharaya, P. Chien, K. Prehoda, B. Tu, J. Weissman, and A. Zarrinpar for advice and helpful comments on the manuscript.

REFERENCES

1. Ranganathan, R., and Ross, E. M. (1997) *Curr. Biol. 7*, R770−3.
2. Craven, S. E., and Bredt, D. S. (1998) *Cell 93*, 495−8.
3. Fanning, A. S., and Anderson, J. M. (1999) *J. Clin. Invest. 103*, 767−72.
4. Schultz, J., Copley, R. R., Doerks, T., Ponting, C. P., and Bork, P. (2000) *Nucleic Acids Res. 28*, 231−4.
5. Schultz, J., Milpetz, F., Bork, P., and Ponting, C. P. (1998) *Proc. Natl. Acad. Sci. U.S.A. 95*, 5857−64.
6. Tsunoda, S., Sierralta, J., Sun, Y., Bodner, R., Suzuki, E., Becker, A., Socolich, M., and Zuker, C. S. (1997) *Nature 388*, 243−9.
7. Gomperts, S. N. (1996) *Cell 84*, 659−62.
8. Kaech, S. M., Whitfield, C. W., and Kim, S. K. (1998) *Cell 94*, 761−71.
9. Saras, J., and Heldin, C. H. (1996) *Trends Biochem. Sci. 21*, 455−8.
10. Songyang, Z., Fanning, A. S., Fu, C., Xu, J., Marfatia, S. M., Chishti, A. H., Crompton, A., Chan, A. C., Anderson, J. M., and Cantley, L. C. (1997) *Science 275*, 73−7.
11. Fuh, G., Pisabarro, M. T., Li, Y., Quan, C., Lasky, L. A., and Sidhu, S. S. (2000) *J. Biol. Chem. 275*, 21486−91.
12. Schepens, J., Cuppen, E., Wieringa, B., and Hendriks, W. (1997) *FEBS Lett. 409*, 53−6.
13. Doyle, D. A., Lee, A., Lewis, J., Kim, E., Sheng, M., and MacKinnon, R. (1996) *Cell 85*, 1067−76.
14. Daniels, D. L., Cohen, A. R., Anderson, J. M., and Brünger, A. T. (1998) *Nat. Struct. Biol. 5*, 317−25.
15. Morais Cabral, J. H., Petosa, C., Sutcliffe, M. J., Raza, S., Byron, O., Poy, F., Marfatia, S. M., Chishti, A. H., and Liddington, R. C. (1996) *Nature 382*, 649−52.
16. Christopherson, K. S., Hillier, B. J., Lim, W. A., and Bredt, D. S. (1999) *J. Biol. Chem. 274*, 27467−73.
17. Brenman, J. E., Chao, D. S., Xia, H., Aldape, K., and Bredt, D. S. (1995) *Cell 82*, 743−52.
18. Garthwaite, J., Charles, S. L., and Chess-Williams, R. (1988) *Nature 336*, 385−8.
19. Bredt, D. S., and Snyder, S. H. (1990) *Proc. Natl. Acad. Sci. U.S.A. 87*, 682−5.
20. Hillier, B. J., Christopherson, K. S., Prehoda, K. E., Bredt, D. S., and Lim, W. A. (1999) *Science 284*, 812−5.
21. Rodnina, M. V., Pape, T., Fricke, R., Kuhn, L., and Wintermeyer, W. (1996) *J. Biol. Chem. 271*, 646−52.
22. Jagath, J. R., Rodnina, M. V., Lentzen, G., and Wintermeyer, W. (1998) *Biochemistry 37*, 15408−13.
23. Creighton, T. E. (1989) *Protein Structure: A Practical Approach*, IRL Press, Oxford, U.K.
24. Gee, S. H., Sekely, S. A., Lombardo, C., Kurakin, A., Froehner, S. C., and Kay, B. K. (1998) *J. Biol. Chem. 273*, 21980−7.
25. Wang, P., Zhang, Q., Tochio, H., Fan, J. S., and Zhang, M. (2000) *Eur. J. Biochem. 267*, 3116−22.
26. Tochio, H., Mok, Y. K., Zhang, Q., Kan, H. M., Bredt, D. S., and Zhang, M. (2000) *J. Mol. Biol. 299*, 359−70.
27. Xu, X. Z., Choudhury, A., Li, X., and Montell, C. (1998) *J. Cell Biol. 142*, 545−55.
28. Fouassier, L., Yun, C. C., Fitz, J. G., and Doctor, R. B. (2000) *J. Biol. Chem. 275*, 25039−45.
29. Schultz, J., Hoffmüller, U., Krause, G., Ashurst, J., Macias, M. J., Schmieder, P., Schneider-Mergener, J., and Oschkinat, H. (1998) *Nat. Struct. Biol. 5*, 19−24.

BI010142L